JOURNAL OF SOLID STATE CHEMISTRY 90, 155–167 (1991)

The Influence of Internal Strain on the Charge Distribution and Superconducting Transition Temperature in $Ba_2YCu_3O_x$

I. D. BROWN

Institute for Materials Research, McMaster University, Hamilton, Ontario, Canada L8S 4M1

Received June 4, 1990; in revised form September 24, 1990

The bond lengths in $Ba_2YCu_3O_x$ expected from chemical considerations alone are not compatible with the constraints imposed by the crystal structure. The resulting strain in the bond lengths can be relaxed *inter alia* by charge transfer between the two Cu atoms. The effect of the strain and its relaxation is examined using bond valences to model the structure at various compositions. At $x = 7.0$ the structure adapts by transferring charge between the two crystallographically distinct Cu atoms to give each an oxidation state of about 2.3. At $x = 6.0$ this mechanism is less effective and the structure contains residual internal strains (Ba–O bonds stretched and Cu–O bonds compressed). Between these limits the charge distribution is determined by crystallographic restrictions on the bond lengths. The predictions of the model agree with two recent systematic studies of the structure and are used to show that the 60 K plateau in T_c results from the ordering that occurs at $x = 6.5$ and that the 90 K plateau is associated with the saturation of T_c as a function of hole concentration. © 1991 Academic Press, Inc.

1. Introduction

$Ba_2YCu_3O_x$ can be thought of as composed of alternating AO (A = Ba, Y) and CuO_2 layers in which some of the O atoms are missing (Fig. 1).

The metal–oxygen distances within the layers are essentially determined only by the a and b lattice spacings: viz. $a = \sqrt{2}$ (AO) = 2(CuO).[1] Oxygen atoms are completely missing from both the Y layer and, at $x = 6.0$, the Cu1 layer, leaving the a axis to be determined only by the Ba–O1 and the Cu2–O2/3 distances. The requirement of commensurability between these two layers constrains the ratio of the bond lengths of Ba–O1 and Cu2–O2/3 to be $\sqrt{2}$, even though chemical considerations would, in general, predict bond lengths with a different ratio. In forcing the layers to be commensurate, the bonds are strained. It is the purpose of this paper to show that the strain is relieved, in part, by charge transfer between the two Cu atoms. By considering the effects of the crystallographic constraints on the bond lengths, one can predict the Cu oxidation states and hence the temperature at which a particular composition becomes superconducting.

The structures are modelled using bond valences following the approach used in earlier studies (*1*, *2*). The present work is extended in three respects. First, these predictions are compared with the results of two new experimental studies by Jorgensen *et al.* (*3*) and Cava *et al.* (*4*) that explore in a

[1] In this study the small difference between a and b in the orthorhombic form is ignored and any observed values are averaged.

0022-4596/91 $3.00

Copyright © 1991 by Academic Press, Inc.
All rights of reproduction in any form reserved.

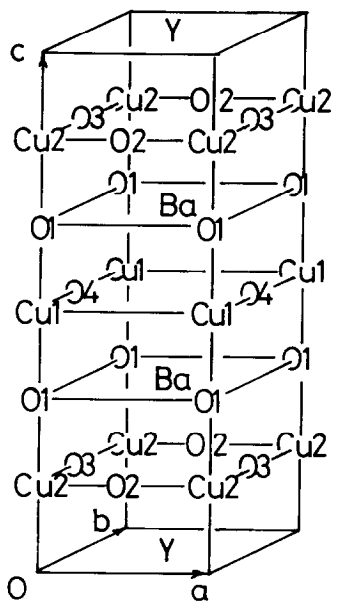

Fig. 1. Structure of $Ba_2YCu_3O_7$ showing the labeling of atoms.

systematic way the changes in structure as the oxygen content is varied. Second, the modelling is used to show that the oxidation states of the Cu atoms are determined by the crystallographic constraints on the structure, and third the relation between the hole concentration and the superconducting transition temperature, T_c, is shown to provide an explanation for the observed variation of T_c with composition.

In the bond valence model (*5*), the atomic valence (or oxidation state) of an atom is assumed to be distributed between the bonds that it forms. As a result, the sum of the valences of the bonds formed by any atom is equal to its atomic valence (see Eq. (7) below). The usefulness of this rule lies in the correlation observed between the length (R) and the valence (s) of a bond as expressed by Eq. (1)

$$s = \exp((R_0 - R)/B), \qquad (1)$$

where $B = 0.37$ Å and R_0 represents the length of a bond of unit valence.

Equation (1) offers a means of using the bond lengths to determine the distribution of charge between the Cu atoms in $Ba_2YCu_3O_x$, but the process is not completely straightforward for three reasons, each of which requires a correction to be made.

(1) The parameters, R_0, have been determined for structures at room temperature. Bond lengths determined at other temperatures must be corrected to room temperature. This correction is described in Section 2.2

(2) The values of R_0 themselves depend on the oxidation state, which is not initially known. A procedure that can be used in these circumstances is described in Section 2.3.

(3) If the bonds lengths are strained they will not correlate properly with the bond valence. Hence Eq. (1) will not give a true measure of the bond valence, even though the bond lengths are accurately known. A procedure used to correct for the effects of strain is described in Section 2.4.

Once these corrections have been applied, a consistent picture of the charge on each Cu atom emerges. The nature of this distribution and its correlation with T_c are discussed in Section 3.

The second part of the paper (Section 4) describes the use of bond valences to model the structures at different compositions. At $x = 6$ (Section 4.2) considerable internal strain remains because the charge redistribution necessary to relax the strain results in unrealistic Cu oxidation states. This is not the case at $x = 7$ (Section 4.3) where the strain in the Cu–O bonds is almost entirely relieved. At intermediate compositions the structure can be modelled by assuming that the added oxygen is either disordered (Section 4.4) or ordered (Section 4.5). The models give good predictions for the observed oxidation states and provide evidence, discussed in Section 5, to support the idea that the plateau region in the T_c vs x curve is associated with the ordered phase of composition $Ba_2YCu_3O_{6.5}$.

2. Analysis of the Observed Structure

2.1 Introduction

In each of the experimental studies of the structure (*3*, *4*) about a dozen samples with different oxygen content were prepared, and the composition and structure of each was accurately determined. However, the samples were prepared in different ways. Jorgensen *et al.* (*3*) prepared their materials by a liquid nitrogen quench of samples that had been annealed at 520°C in atmospheres with a well-controlled oxygen partial pressure. Cava *et al.* (*4*) prepared their samples by gettering with Zr at 440°C. Both determined the structures by neutron powder diffraction but Jorgensen *et al.* made their measurements at room temperature while Cava *et al.* made theirs at 5°K. The difference in measurement temperatures results in smaller lattice parameters being reported by Cava *et al.* In addition, the tetragonal to orthorhombic transition is less abrupt in the quenched samples than in the gettered ones, as shown both by the lattice parameters (Fig. 2) and the ordering of O4.

2.2 Correction for Temperature

To make a direct comparison between the two sets of structures, the lattice parameters found in the low temperature study of Cava *et al.* were multiplied by factors (shown in Table I) that were designed to fit them to the lattice parameters of Jorgensen *et al.*, at $x = 7$ and $x = 6$.

TABLE I

FACTORS USED TO MULTIPLY THE LATTICE PARAMETERS OF CAVA *et al.* (*4*) TO CORRECT FOR TEMPERATURE

	Orthorhombic phase	Tetragonal Phase
a	1.0024	1.0013
b	1.0007	
c	1.0017	1.0006

Because of the paucity of measurements in the region close to $x = 6.0$, there is some uncertainty about the size of the corrections applied to the tetragonal phase. The variation of the corrected lattice parameters with oxygen content is shown in Fig. 2.

2.3 Calculation of the Bond Valences

Oxidation states were determined from the observed bond lengths using the bond valence model (*5*). Bond valences were calculated from the bond lengths using Eq. (1). The values of R_0 used for Ba–O and Y–O bonds were 2.285 and 2.019 Å, respectively (*6*) but the value used for the Cu–O bonds depended on oxidation state. Values for the integral oxidation states are taken from an earlier paper (*2*): 1.600 Å (Cu^+), 1.679 Å (Cu^{2+}) and 1.739 Å (Cu^{3+}). A linear interpolation between these values was used for intermediate oxidation states.[2]

Because R_0 depends on oxidation state, the oxidation states of the two Cu atoms must be known before the bond valences can be calculated. However, the bond valences are needed in order to determine the oxidation states. This problem was solved using the procedure developed earlier (*2*). Valences (s'') were calculated assuming that the copper was Cu^{2+}. The bond valence sum ($V'' = \Sigma s''$) around a Cu atom was used to determine whether its oxidation state was greater than or less than 2. If it was greater, the proportion (y) of Cu^{3+} on the site was calculated using Eq. (2)

$$y = (V'' - 2)/(V'' + 1.0 - V''') \quad (2)$$

and, if less, the proportion of Cu^{2+} (z) was calculated using Eq. (3),

$$z = (V' - 1)/(V' + 1.0 - V''), \quad (3)$$

[2]The assumption of a formal copper valence of +3 does not imply that the electron holes are physically present on the Cu atom. As shown previously (*2*), the bond valence model is insensitive to the location of the holes, but placing the formal charge on Cu simplifies the calculations.

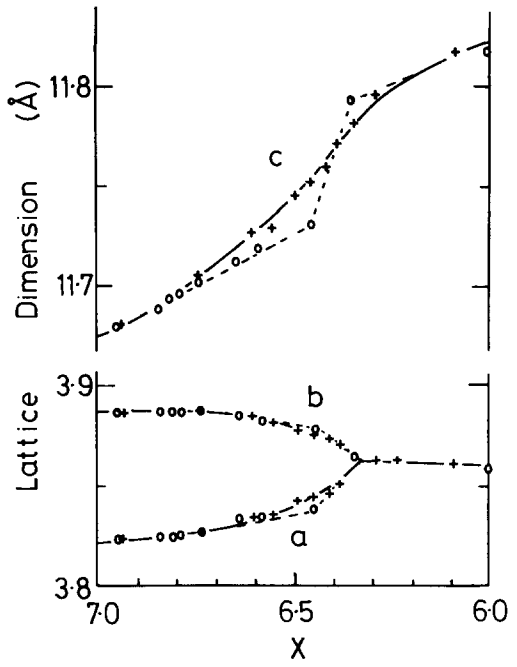

Fig. 2. Lattice dimensions as a function of x. Crosses, annealed samples (*3*); circles, gettered samples (*4*) corrected to room temperature.

where V' is the valence sum calculated by assuming the copper is Cu^+ and V''' the valence sum calculated assuming the copper is Cu^{3+}. In the absence of internal strain in the crystal (see below) the correct oxidation state is given as either $1.0 + z$ or $2.0 + y$.

2.4 Strain Correction

The bond valence sum around each atom is expected to be equal to its formal oxidation state, but the sums around Ba, O1, and the average sum around the two Cu atoms calculated using the procedure described above, are found to differ from this value systematically with x. This difference has been attributed to internal strains within the structure: the Ba atom is too large for the Cu–O framework at $x = 7$ and too small at $x = 6$ (*2*). Consequently the apparent oxidation states of Ba and O1 at $x = 6.0$ are too small and the average oxidation state calculated for Cu is too large. To get a true picture of the Cu oxidation states, the charge indicated by the bond valence sums must be corrected for strain to ensure that the total charge over all Cu atoms is equal to that expected from stoichiometry.

The following procedure was used. Initial values of the oxidation states ("apparent oxidation states") were estimated using the procedure described in Section 2.3. These values were not correct because (a) the bond lengths on which they are based suffer from internal strain and (b) the true value of R_0 was not known because the true oxidation state was not known at this stage. However, the differences between the apparent oxidation states and those calculated from the stoichiometry give a measure of the strain correction that must be applied. For Cu, only the average charge on the three Cu atoms in the formula unit can be calculated from the stoichiometry, which means that only an average correction for Cu can be found. The effect of the strain on the average valence sum is shown in Fig. 3 (curve A for Ba and curves B and C for Cu), which shows the difference between the valence sums and the oxidation states determined from the stoichiometry.

The correction that must be applied to the valence sums of Cu is given in analytical form in Eq. (4) for the gettered samples (*4*) and Eq. (5) for the quenched samples (*3*),

$$d = 0.26(x - 6.72) \text{ valence units (v.u.)} \quad (4)$$

$$d = 0.23(x - 6.68) \text{ v.u.} \quad (5)$$

Application of these corrections to the apparent oxidation states then gives the "true oxidation states." These were assumed to be correct since they correspond to the observed stoichiometry, but the assumption that both kinds of copper atom are equally strained is arbitrary and could

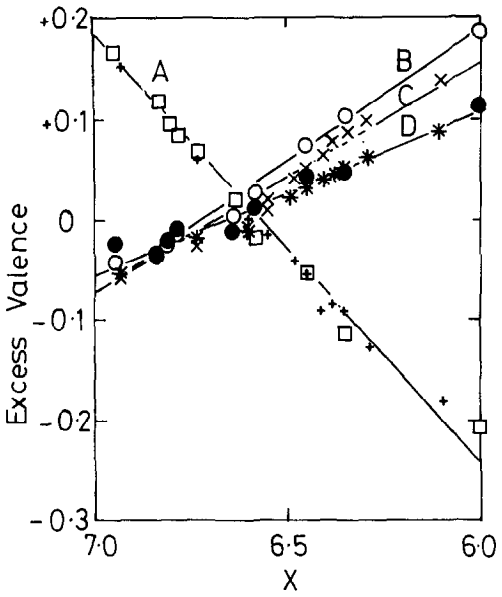

Fig. 3. The internal strain expressed as the difference between the valence sums and the expected oxidation states. A: Ba, + = Ref. (*3*), squares = Ref. (*4*); B: Cu (average using apparent valences), circles = Ref. (*4*); C: Cu (average using apparent valences), X = Ref. (*3*) D: Cu (average using true valences), * = Ref. (*3*), filled circles = Ref. (*4*).

lead to an error as large as 0.1 v.u. in the proposed oxidation states at $x = 6.0$. At most other compositions in error is much smaller and can be neglected.

Once the true oxidation states were determined, a new set of bond valences was calculated using the value of R_0 appropriate to the true oxidation state. Even though these bond valences were calculated using the correct value of R_0 they were, of course, still not correct, in the sense of giving valence sums equal to the oxidation states, since they were calculated from observed bonds lengths uncorrected for strain. No attempt was made to correct individual bond lengths or bond valences for strain as this would have required assumptions to be made about the way in which the strain is distributed between the bonds.

The differences between the oxidation states of Cu and the valence sums calculated with the "true" values of R_0 are shown by line D in Fig. 3. They correspond to the true strain corrections and are given for both sets of samples by d' in Eq. (6).

$$d' = 0.16(x - 6.66) \text{ v.u.} \qquad (6)$$

This is the correction used for the bond lengths predicted by the models described in Section 4.

3. Results of the Analysis of the Observed Structures

The oxidation states found are shown in Fig. 4 by crosses for the quenched samples and by open figures for the gettered samples.

The lines in this figure correspond to the model discussed in Section 4.4 below. Curve A gives the oxidation state of Cu1

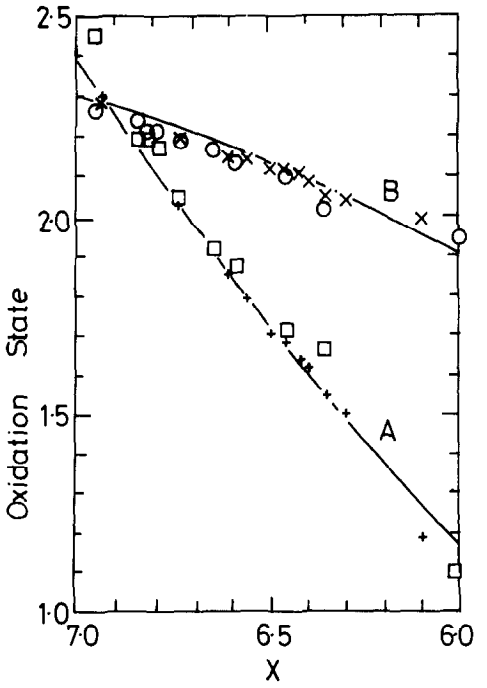

Fig. 4. Oxidation states: for Cu1, A = predicted; + = Ref. (*3*); squares = Ref. (*4*); for Cu2; B = predicted; X = Ref. (*3*); circles = Ref. (4).

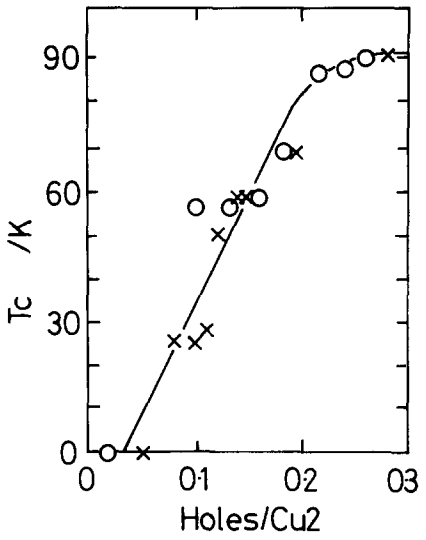

Fig. 5. Superconducting transition temperature as a function of hole concentration at Cu2. X = Ref. (*3*), circles = Ref. (*4*).

and curve B the oxidation state of Cu2. Both sets of samples show a steady increase in oxidation state as x increases for both copper atoms, but the gettered samples in particular show small kinks near x = 6.35, associated with the tetragonal to orthorhombic phase transition, and near x = 6.8 associated with the loss of ordering.

Cava *et al.* (*4*) point out that the variation in the oxidation state of Cu2 with x follows closely the variation of the superconducting transition temperature, T_c. Both graphs show rapid increases at x = 6.35 and x = 6.8 and are relatively flat in between. This correlation is less apparent with the true oxidation states than it is with the uncorrected valence sums shown in Fig 16, of Ref. (*4*), a point that will be discussed in Section 5 below. Nevertheless, there is a correlation between T_c and the oxidation state (hole concentration) of Cu2 as shown in Fig. 5 and it is similar to the correlation found by Tokura *et al.* (*7*) in doped samples of $Ba_2YCu_3O_x$.

Between 0.04 and 0.22 holes/Cu, T_c increases by 500 K/(hole/Cu) but beyond 0.22 holes/Cu it levels off to a constant 90 K. Beyond 0.3 holes/Cu Tc is expected once again to fall.

A similar bond valence analysis of the experiments of Cava *et al.* and Jorgensen *et al.* by Tallon (*8*) comes to a similar conclusion but, as he did not correct the bond valence sums for strain and estimates the charges on Cu2 in a different way, his quantitative estimates of the hole concentrations are low.

4. Modelling the Structure

4.1 Method

Bond valences were used to model the structures in a manner similar to that used in the earlier study (*2*). Ideal bond lengths are predicted by solving the bond network for bond valences using the two Kirchhoff-like network Eqs. (7) and (8).

$$\Sigma_j s_{ij} = V_i \tag{7}$$

$$\Sigma_{\text{loop}} s_{ij} = 0, \tag{8}$$

where s_{ij} is the valence of the bond between atoms i and j and V_i is the oxidation state of atom i. In the loop equation the bonds are taken to be positive if traversed from oxygen to the metal and negative if traversed in the opposite direction. These equations have been found to give good predictions of bond valences (and hence bond lengths) in most inorganic compounds in which strain is not present and electronic effects do not distort the atomic environments. To allow for the Jahn–Teller distortion of the environment of Cu2, it was necessary to fix the valence of the Cu2–O1 bond arbitrarily, but the numerical predictions of the model are not very sensitive to the exact choice of this value. The values chosen lie between 0.1 (x = 6.0) and 0.2 v.u. (x = 7.0), values typical of those found for the axial bond in Cu^{2+} environments. The difference between the modelled bond lengths and those observed

TABLE II

BOND VALENCES, BOND LENGTHS, AND BOND VALENCE SUMS FOR THE IDEAL AND OBSERVED STRUCTURES OF $Ba_2YCu_3O_6$ (SEE THE TEXT FOR DETAILS). UNDERLINED QUANTITIES ARE THOSE ASSUMED

Cu2 oxidation:	A 1.00	B 1.35	C 1.60	D 2.00	E 2.00	F observed	G strain E–D	H relax F–E
				Bond valences				
Cu1–O1	1.500	1.150	0.900	0.500	0.500	0.616	0.0	+0.116
Cu2–O1	0.100	0.100	0.100	0.100	0.100	0.116	0.0	+0.116
Cu2–O2	0.225	0.313	0.375	0.475	0.515	0.485	+0.040	−0.030
Ba–O1	0.100	0.188	0.250	0.350	0.310	0.265	−0.040	−0.045
Ba–O2	0.400	0.312	0.250	0.150	0.150	0.183	0.0	+0.033
				Bond lengths (Å)				
Cu1–O1	1.589	1.645	1.702	1.856	1.856	1.787	0.0	−0.069
Cu2–O1	2.452	2.480	2.299	2.531	2.531	2.471	0.0	−0.060
Cu2–O2	2.152	2.058	2.010	1.954	1.925	1.943	−0.029	+0.038
Ba–O1	3.137	2.903	2.798	2.673	2.718	2.777	+0.045	+0.059
Ba–O2	2.624	2.716	2.798	2.987	2.987	2.914	0.0	−0.073
				Bond valence sums				
Cu1	3.00	2.30	1.80	1.00	1.00	1.23	0.0	+0.23
Cu2	1.00	1.35	1.60	2.00	2.18	2.06	+0.18	−0.12
Ba	2.00	2.00	2.00	2.00	1.84	1.79	−0.16	−0.50
O1	2.00	2.00	2.00	2.00	1.84	1.79	−0.16	−0.05
O2	2.00	2.00	2.00	2.00	2.09	2.05	+0.09	−0.04

Note. A–D, models of the structure that satisfy the valence sum rule using the oxidation states shown. Underlined values are those assumed. The Y–O bonds (not shown) are assumed to be 0.375 v.u. in all models. E, model D with the Ba–O1 and Cu2–O2 bonds modified to fit the predicted lattice parameter a = 3.844 Å. F, observed values (uncorrected for strain) of the gettered sample (*4*). G, strain introduced in changing model D to model E. H, relaxation between the strained structure (column E) and that observed (column F).

is assumed to give a measure of the strain and its relaxation.

4.2 Modelling the Structure at x = 6.0

To determine the ideal structure at x = 6.0, it is only necessary to assume oxidation states for Cu1 and Cu2 and to assume that the Cu2–O1 bond has a valence of 0.1 v.u. The results are given in Table II for several possible oxidation states.

Values of the a lattice parameter predicted using these ideal Ba–O1 and Cu2–O2 bond lengths (ignoring the small effect of the layer puckering) are shown in Fig. 6a and indicate that, for commensurability be-

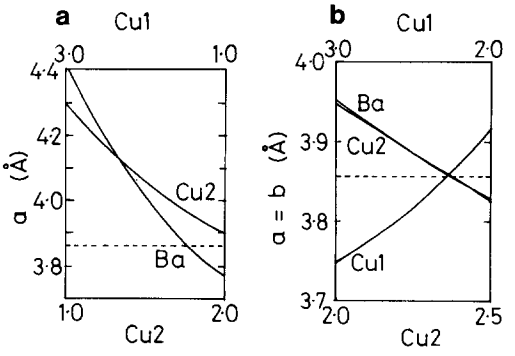

Fig. 6. Ideal a axis length expected for the BaO, CuO, and CuO_2 layers as a function of the distribution of charge on the Cu atoms. The broken line gives the observed value of a (a) at x = 6.0; (b) at x = 7.0

tween the BaO and CuO_2 layers, the oxidation state of Cu2 should be 1.35 and that of Cu1 2.30, a distribution that is incompatible with the observed coordination environments around copper (linear coordination for monovalent copper and square planar or tetragonally distorted octahedral coordination for di- or trivalent copper).

The oxidation states expected from the coordination environments (Cu1 = +1 and Cu2 = +2 (Table II, column D)) give Ba–O1 and Cu2–O2 distances that are incommensurate since they have a ratio of only 1.368 rather than 1.414 (= $\sqrt{2}$) as required by the crystal structure. Strain in these bonds is therefore inevitable. To fit the bond lengths to a common value of a the Ba–O1 bond must be stretched and the Cu2–O2 bond must be compressed. The mean predicted a for the two layers, 3.84 Å, is close to the observed length, 3.86 Å (shown by the broken line in Fig. 6a), indicating that the Ba and Cu environments are equally strained. If one adjusts the Ba–O1 and Cu2–O2 bond lengths of model D to fit a = 3.84 Å, one gets the model shown in column E of Table II. For comparison column F shows the values observed by Cava *et al.* (*4*). The strain required for commensurability (the difference between columns D and E) is given in column G, and the relaxation of the strained structure (the difference between columns E and F) is given in Column H. Puckering of the layers, itself a result of crystallographic constraints in the c direction, tends to increase the intralayer bond lengths but the interlayer relaxations shown in Column H suggest that there is a transfer of about 0.1 holes from each Cu2 to Cu1.

4.3 Modelling the Structure at x = 7.0

The ideal structure for x = 7.0 was calculated with the Cu2–O1 bond fixed at 0.2 v.u. Again several different charge distributions were examined. The results are given in Table III and the predicted axis lengths, a (assumed equal to b), are shown in Fig. 6b for each of the three layers (CuO, BaO, and CuO_2). The match between the CuO_2 and the BaO layers is close at all charge distributions and all three predicted values of a are the same when the oxidation states of both Cu1 and Cu2 are about 2.33 corresponding to a = 3.85 Å (c.f., the observed average of a and b = 3.855 Å given by the broken line in Fig. 6b). Comparing the ideal structure (Table III, column B) with the observed structures (columns E (x = 6.93) and F (x = 6.95)) suggests that the oxidation state of Cu1 is probably a little larger than 2.33 and that of Cu2 a little less.

4.4 Modelling the Charge Distribution for $6.0 < x < 7.0$

For intermediate values of x it is not possible to use the method of Section 4.1 to model the structure without knowing the distribution of oxygen over the O4 sites. Consequently an alternative method was used.

Assume that the valence of the Cu1–O1 bond remains constant at 0.65 v.u. Although the length of this bond is observed to increase with x, this increase is almost exactly compensated by the change in R_0 as the oxidation state of Cu1 increases, so that its valence remains close to 0.65 as shown in Fig. 7. There are, however, small but significant deviations from this value that will be discussed later.

Since the deviations are small, the primary contribution to the increase in the oxidation state of Cu1 comes from the increase in the number of O4 atoms in its average coordination sphere. The length of the Cu1–O4 bond depends only on the b lattice dimension and is essentially constant at 1.930 Å over the whole composition range. Its valence (s), however, increases with x because of the increase in R_0 with oxidation state. Equation (9) represents a linear interpolation between the valence of a bond of length 1.930 Å formed by Cu^+ at x = 6.0

TABLE III

IDEAL BOND VALENCES, BOND LENGTHS AND BOND VALENCE SUMS CALCULATED FOR THE STRUCTURE WITH $x = 7.0$; THE VALENCE OF Cu2–O1 IS TAKEN AS 0.2 AND VARIOUS DISTRIBUTIONS OF CHARGE ARE ASSUMED

Cu2 charge:	A 2.50	B 2.33	C 2.167	D 2.00	E ref *4*	F ref *3*
			Bond valences			
Cu1–O1	0.527	0.618	0.709	0.800	0.702	0.649
Cu1–O4	0.472	0.548	0.624	0.700	0.524	0.513
Cu2–O1	0.200	0.200	0.200	0.200	0.191	0.197
Cu2–O2/3	0.575	0.533	0.492	0.450	0.506	0.508
Ba–O1	0.318	0.296	0.273	0.250	0.289	0.291
Ba–O2/3	0.050	0.092	0.133	0.175	0.156	0.154
Ba–O4	0.264	0.226	0.188	0.150	0.201	0.201
			Bond lengths (Å)			
Cu1–O1	1.916	1.876	1.846	1.822	1.836	1.857
Cu1–O4	1.957	1.921	1.893	1.871	1.944	1.944
Cu2–O1	2.303	2.293	2.283	2.274	2.306	2.296
Cu2–O2/3	1.913	1.931	1.950	1.974	1.946	1.946
Ba–O1	2.709	2.735	2.765	2.798	2.744	2.742
Ba–O2/3	3.393	3.168	3.031	2.930	2.972	2.976
Ba–O4	2.778	2.835	2.903	2.987	2.879	2.879
			Bond valence sums			
Cu1	2.000	2.333	2.667	3.000	2.400	2.246
Cu2	2.500	2.333	2.167	2.000	2.215	2.223
Ba	2.000	2.000	2.000	2.000	2.164	2.156
O1	2.000	2.000	2.000	2.000	2.049	2.040
O2/3	2.000	2.000	2.000	2.000	2.040	2.058
O4	2.000	2.000	2.000	2.000	1.852	1.828

Note. Columns A–D, models with various assumed charge distributions as shown. Underlined values are those assumed in the calculation. Columns E–F, observed values (uncorrected for strain) for $x = 0.95$ and $x = 0.93$, respectively.

and that of a bond of the same length formed by $Cu^{2.3+}$ and $x = 7.0$.

$$s = 0.410 + 0.123(x - 6). \quad (9)$$

Adding an oxygen atom to the Cu1 layer will add a charge of —2.0 to the crystal, but the two Cu1–O4 bonds that are created will only contribute $2s$ (a value which ranges between 0.82 and 1.07 v.u.) to the bond valence sum at Cu1. The remaining charge is transferred to Cu2. This is reflected in small changes to the Ba–O and Cu2–O bonds, changes which are often masked by the variations in R_0 and the effects of the internal strain, but the charge transfer can be seen in the shortening of the Cu2–O1 bond, the lengthening of the Ba–O2/3 bond and, of course, the increase in the number of Ba–O4 bonds as x increases.

Equation (9) can be used to predict the valence of the Cu1–O4 bond and hence the oxidation state of Cu1 (assuming a constant valence of 0.65 for the Cu1–O1 bond) at various compositions. This prediction, corrected for strain using Eq. (6), is shown as line A in Fig. 4. The stoichiometry and the

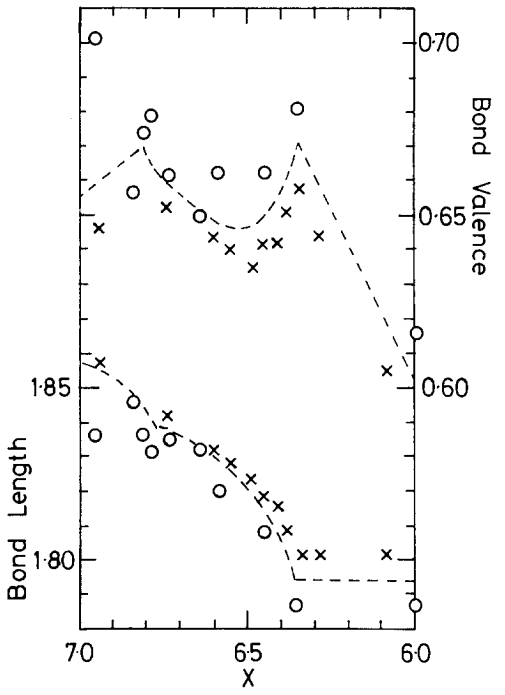

Fig. 7. The valence (top) and length (bottom) of the Cu1–O1 bond as a function of x. X, Ref. (*3*); circles, Ref. (*4*). The line is drawn between the two sets of measurements to aid the eye.

requirement of charge neutrality then permit the oxidation state of Cu2 to be predicted (line B in Fig. 4). The overall agreement between the predicted and observed oxidation states is consistent with the idea that the observed charge distribution results from the requirement that the CuO layer must be commensurate with the BaO and CuO_2 layers.

Closer examination of the observed oxidation states in Fig. 4 shows that they deviate in a small but significant way from the model, particularly with the gettered samples (shown by circles and squares). In particular, the oxidation state of Cu1 increases faster than the model predicts in the tetragonal phase because the length of the Cu1–O1 bond remains constant, leading to its valence increasing as the oxidation state increases (Fig. 7). In the gettered samples the ordering phase transitions occur at the same compositions as the discontinuities in the slope of Fig. 4 (x = 6.35 and 6.80). These discontinuities are associated with, and are seen most clearly in, the valences of the Cu1–O1 bond (Fig. 7).

At the highest values of x, the two samples (x = 6.93 for the quenched sample and x = 6.95 for the gettered sample) differ significantly in the position found for O1, making it difficult to assess the true distribution of the oxidation states in this limit.

4.5 Modelling the Structure at x = 6.5

At x = 6.5 a superstructure is often observed. It is assumed to arise from a structure in which the Cu1 atoms along the a direction are alternately 2- and 4-coordinate. To model this structure, the valence of all the Cu2–O1 bonds was taken as 0.15 v.u. and the oxidation states of the copper atoms were taken as:

Cu1	(4-coordinate)	2.23
Cu1′	(2-coordinate)	1.30
Cu2		2.13,

values which are derived from the model developed in Section 4.4. The results, shown in Table IV, lead to predicted values of a (= b) of 3.870 Å (Cu1 layer), 3.894 Å (Cu2 layer), and 3.830 Å (Ba layer) which average to 3.862 Å for a and 3.865 Å for b (Cu1 does not contribute to a).

These values are midway between the observed values of a = 3.842 Å and b = 3.878 Å and indicate that little strain is needed to ensure commensurability. However, commensurability in the c direction requires that the Cu2–Cu1 distance be close to the Cu2–Cu1′ distance. This is not the case in the model where the Cu2–O1 and Cu2–O1′ distances are assumed to be equal, but the Cu1–O1 and Cu1′–O1′ distances are predicted to differ by 0.1 Å. The strain resulting from forcing Cu2–Cu1 to equal Cu2–Cu1′ can be relieved in at least

TABLE IV

IDEAL BOND VALENCES AND BOND LENGTHS CALCULATED FOR $x = 6.5$.

Bond valences	
Cu1–O1	0.594
Cu1–O4	0.521
Cu1′–O1′	0.650
Cu2–O1	0.150
Cu2–O2/3	0.493
Ba–O1	0.338
Ba–O1′	0.300
Ba–O2/3	0.133
Ba–O4	0.266
Bond lengths (Å)	
Cu1–O1	1.887
Cu1–O4	1.935
Cu1′–O1′	1.783
Cu2–O1	2.389
Cu2–O2/3	1.947
Ba–O1	2.686
Ba–O1′	2.730
Ba–O2/3	3.031
Ba–O4	2.775

Note. The atom Cu1 is 4-coordinate and Cu1′ 2-coordinate. The valences assumed for copper are: Cu1 2.23, Cu1′ 1.30, and Cu2 2.12. The bond valence of Cu2–O1 is taken to be 0.15.

two different ways. In the first, Cu1–O1 would be shortened to match Cu1′–O1′ by lengthening Cu1–O4 to 1.970 Å, i.e. by increasing b by 0.076 Å to 3.941 Å. This is considerably larger than the lengthening required to match the observed value of b (0.013 Å), indicating that this mechanism is of minor importance. The second relaxation mechanism involves changing the lengths of Cu2–O1 and Cu2–O1′, which would result in the Cu2 atoms having different oxidation states depending on whether they are bonded to O1 or O1′. From the bond valence change that is needed to produce the necessary bond length change, one can predict that the Cu2 atoms bonded to O1′ should have an oxidation state of 2.11 v.u. and those bonded to O1 an oxidation state of 2.15 v.u. Assuming that T_c is determined by the Cu2 atoms with the higher hole concentration, one can predict from Fig. 5 that $T_c = 58$ K for this phase, exactly the value found for the plateau region where the ordered structure is found.

5. Discussion

Modelling the structure of $Ba_2YCu_3O_x$ between $x = 6.0$ and $x = 7.0$ using bond valences, shows that the lengths expected for the bonds on chemical grounds lead to layers that are incommensurate. Commensurability can only be achieved by introducing a strain in the bond lengths. There are several mechanisms for relaxing this strain, including changing the interlayer bond lengths and transferring charge between the two Cu atoms. At $x = 6.0$ these mechanisms are not fully effective and some internal strain remains.

An analysis of two recent systematic measurements of the structure as a function of oxygen content shows that the oxidation states of both copper atoms (Cu1 and Cu2) increase as the oxygen content increases (Fig. 4). The increase is almost uniform, though small discontinuities in the slope are visible at the places where changes occur in the ordering of the oxygen atoms ($x = 6.35$ and $x = 6.8$). The superconducting transition temperature correlates well with the hole concentration on Cu2 (Fig. 5), allowing structural models to be used to predict T_c.

Modelling the structures at various oxygen compositions gives an insight into the factors that determine the structure and hence the oxidation states and transition temperatures. At $x = 6.0$ the charges are close to +1 (Cu1) and +2 (Cu2) and there is considerable internal strain. Because there are no holes in the Cu2 plane (the oxidation state of Cu2 is less than 2.0) the compound is not superconducting. Adding oxygen in a way that preserves commensurability requires that the charges of both Cu1 and Cu2 increase. At around $x = 6.2$, holes first ap-

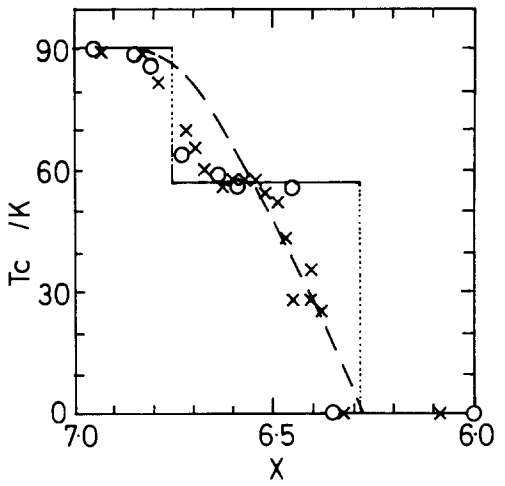

Fig. 8. Superconducting transition temperature as a function of x. X, Ref. (*3*); circles, Ref. (*4*). The solid line gives T_c predicted for a maximally ordered structure, the broken line is for a fully disordered structure.

pear in the Cu2 layer and around $x = 6.3$, the hole concentration reaches the critical value for superconductivity. Simultaneously the oxygen content reaches a level at which the ordered $Ba_2YCu_3O_{6.5}$ phase, which is predicted to have $T_c = 58$ K, first appears. A rapid increase in T_c with x is therefore expected in this region. Although the average charge on Cu2 continues to increase monotonically with x, T_c is controlled by the major phase present. Only when the order breaks down and extensive regions with the $Ba_2YCu_3O_7$ structure appear at $x = 6.8$ does Tc once again rise to its maximum value of 90 K.

The observed variation of T_c with x is shown in Fig. 8 by circles for the gettered samples (*4*) and crosses for the annealed samples (*3*).

The lines are predictions based on the structural models and on the hole/T_c correlation shown in Fig. 5. The solid line gives the value of T_c expected for the major phase in a crystal that is composed only of the three ordered structures modelled above. The broken line corresponds to T_c predicted for the fully disordered model developed in Section 4.4. The plateau region at around 60 K, which is broader in the more ordered samples of Cava *et al.* (*4*), can be identified with the presence of the ordered $x = 6.5$ phase. By contrast the plateau with $T_c = 90$ K at $x = 7.0$ is the result of the saturation of T_c as the hole concentration exceeds 0.2 per copper. Further increases in hole concentration are expected to result in a decrease in T_c.

Changes in pressure are predicted and found (*9*) to force O1 to lie more centrally between Cu1 and Cu2 since this will shorten the Cu1–Cu2 distance. The effect of this movement is to transfer holes to Cu2. For compositions with $x < 6.7$ an increase in hole concentration is expected to result in an increase of T_c (Fig. 5), but for higher O content there should be little change in Tc as observed by Shirber *et al.* (*10*) and Chu *et al.* (*11*).

Acknowledgments

I thank R. J. Cava and J. D. Jorgensen for their encouragement, Aniceta Skowron for helpful discussions, and the Natural Science and Engineering Research Council of Canada for financial support.

References

1. M. O'Keeffe, and S. Hansen, *J. Amer. Chem. Soc.* **110,** 1506 (1988).
2. I.D. Brown, *J. Solid State Chem.* **82,** 122 (1989).
3. J. D. Jorgensen, B. W. Veal, A. P. Paulikas, L. J. Nowicki, G. W. Crabtree, H. Claus, and W. K. Kwok, *Phys. Rev. B* **41,** 1863 (1990).
4. R. J. Cava, A. W. Hewat, E. A. Hewat, B. Batlogg, M. Marezio, K. M. Rabe, J. J. Krajewski, W. F. Peck Jr., and L. W. Rupp Jr., *Physica C* **165,** 419 (1990).
5. I. D. Brown, *Phys. Chem. Mineral.* **15,** 30 (1987).

6. I. D. BROWN, AND D. ALTERMATT, *Acta Crystallogr.* **B41,** 244 (1985).
7. Y. TOKURA, J. B. TORRANCE, T. C. HUANG, AND A. I. NAZZAL, *Phys. Rev. B* **38** 7156 (1988).
8. J. L. TALLON, *Physica C* **168,** 85 (1990).
9. J. D. JORGENSEN, S. PEI, P. LIGHTFOOT, D. G. HINKS B. W., VEAL, B. DABROWSKI, A. P. PAULIKAS, R. KLEB, AND I. D. BROWN, to be published (1990).
10. J. E. SCHIRBER, D. S. GINLEY, E. L. VENTURINI, AND B. MOROSIN, *Phys. Rev. B* **35,** 8709 (1987).
11. C. W. CHU, Z. J. HUANG, R. L. MENG, L. GAO, AND P. H. HOR, *Phys. Rev. B* **37,** 293 (1988).